Role for Drs2p, a P-Type ATPase and Potential Aminophospholipid Translocase, in Yeast Late Golgi Function

Chih-Ying Chen, Michael F. Ingram, Peter H. Rosal, and Todd R. Graham

Department of Molecular Biology, Vanderbilt University, Nashville, Tennessee 37235

Abstract. ADP-ribosylation factor appears to regulate the budding of both COPI and clathrin-coated transport vesicles from Golgi membranes. An *arf1Δ* synthetic lethal screen identified *SWA3/DRS2*, which encodes an integral membrane P-type ATPase and potential aminophospholipid translocase (or flippase). The *drs2* null allele is also synthetically lethal with clathrin heavy chain (*chc1*) temperature-sensitive alleles, but not with mutations in COPI subunits or other *SEC* genes tested. Consistent with these genetic analyses, we found that the *drs2Δ* mutant exhibits late Golgi defects that may result from a loss of clathrin function at this compartment. These include a defect in the Kex2-dependent processing of pro–α-factor and the accumulation of abnormal Golgi cisternae. Moreover, we observed a marked reduction in clathrin-coated vesicles that can be isolated from the *drs2Δ* cells. Subcellular fractionation and immunofluorescence analysis indicate that Drs2p localizes to late Golgi membranes containing Kex2p. These observations indicate a novel role for a P-type ATPase in late Golgi function and suggest a possible link between membrane asymmetry and clathrin function at the Golgi complex.

Key words: adenosine diphosphate–ribosylation factor • aminophospholipid translocase • clathrin • DRS2 • trans-Golgi network

The directed movement of proteins between compartments of the secretory and endocytic pathways is driven by the formation of small coated transport vesicles that bud from a donor compartment, and then fuse with an acceptor compartment. COPI, COPII, and clathrin are the best characterized coat proteins involved in protein transport. COPI, a heptameric (α, β, β′, γ, δ, ϵ, ζ-COP) protein complex, coats vesicles that mediate protein transport from the Golgi to the ER and possibly between Golgi compartments. To initiate budding of COPI-coated vesicles from Golgi membranes, the small GTP-binding protein ADP-ribosylation factor (ARF)[1] mediates the recruitment of COPI coats to primarily cis Golgi cisternae. ARF is also required to recruit clathrin/AP-1 coats to the trans-Golgi network. Clathrin coats are assembled from triskelions composed of three clathrin heavy chains and three light chains. The tetrameric adaptor protein (AP) complex, AP-1, links membrane proteins to clathrin at the TGN and appears to facilitate cargo delivery to endosomal compartments (reviewed in Schmid, 1997). Interestingly, the molecular basis for the ARF-dependent recruitment of COPI and clathrin/AP-1 to two different regions of the Golgi complex is not known. Clathrin/AP-2 vesicles mediate the internalization of proteins from the plasma membrane, although recruitment of this coat does not appear to require ARF. In addition, the recruitment of COPII to ER membranes is mediated by the small GTP-binding protein Sar1p rather than ARF.

In yeast *Saccharomyces cerevisiae,* ARF is encoded by two nearly identical genes, *ARF1* and *ARF2*, that appear to be functionally redundant. Deletion of both *ARF* genes is lethal, but strains harboring either an *arf1Δ* or an *arf2Δ* allele are viable and grow nearly as well as an isogenic wild-type strain (Stearns et al., 1990a). However, deletion of the more highly expressed *ARF1* gene causes a defect in the kinetics of protein transport through the secretory pathway, a reduction in Golgi-dependent glycosylation of secreted glycoproteins, and substantial changes in the morphology of Golgi cisternae and endosomes (Gaynor et al., 1998; Stearns et al., 1990b).

To gain a better understanding of the essential role that ARF plays in vivo, we have used a genetic screen to identify seven genes (*SWA1–SWA7*) for which mutant alleles

Drs. Chen and Ingram contributed equally to this work and should be considered co–first authors.

Address correspondence to Todd R. Graham, Department of Molecular Biology, Vanderbilt University, Nashville, TN 37235. Tel.: (615) 343-1835. Fax: (615) 343-6707. E-mail: tr.graham@vanderbilt.edu

1. *Abbreviations used in this paper:* AP, adaptor protein; ARF, ADP-ribosylation factor; CCV, clathrin-coated vesicle; CPY, carboxypeptidase Y; EM, electron microscopy; HA, hemagglutinin; ORF, open reading frame; PE, phosphatidylethanolamine; PS, phosphatidylserine; ts allele, temperature-sensitive allele.

exhibit synthetic lethality with *arf1Δ*. This genetic interaction often predicts that the two gene products function in the same pathway or in parallel pathways. *swa5-1* was previously identified as a new temperature-sensitive (ts) allele of the clathrin heavy chain gene (*chc1-5*), providing support for a functional interaction in vivo between clathrin and ARF (Chen and Graham, 1998). Deletion of the *CHC1* gene can be lethal or viable depending on the strain background. Mutants harboring *chc1Δ*, if viable, exhibit slow growth, decreased rates of endocytosis, and a defect in retention of late Golgi membrane proteins (Payne et al., 1987, 1988; Payne and Schekman, 1989; Lemmon et al., 1990). Disruption of the clathrin light chain gene (*CLC1*) causes a reduced stability of Chc1p and results in phenotypes similar to that of *chc1* mutants (Chu et al., 1996). Although mutations in AP-1 subunits (Aps1p, Apm1p, and Apl2p) do not result in any detectable phenotypes, a pairwise combination of *aps1Δ*, *apm1Δ*, or *apl2Δ* with *chc1-ts* exacerbates defects in growth and retention of Golgi resident proteins relative to the *chc1-ts* mutant (Phan et al., 1994; Rad et al., 1995; Stepp et al., 1995).

Here we report that *SWA3* is allelic to *DRS2*, which encodes an integral membrane P-type ATPase (Ripmaster et al., 1993) that is 47% identical to the mammalian ATPase II purified from chromaffin granules (Tang et al., 1996). ATPase II is thought to be an aminophospholipid translocase (Auland et al., 1994; Zachowski et al., 1989), capable of flipping phosphatidylserine (PS) or phosphatidylethanolamine (PE) from the external leaflet of a lipid bilayer to the cytoplasmic leaflet to generate an asymmetric distribution of these lipids in the two leaflets of a membrane. In mammalian cells, most of the plasma membrane PS is restricted to the cytoplasmic leaflet by the action of a similar aminophospholipid translocase, but a calcium influx induces the loss of plasma membrane lipid asymmetry and results in the exposure of PS on the cell surface. This event allows recognition and removal of apoptotic cells by phagocytes, and in blood cells activates the coagulation cascade (Williamson and Schlegel, 1994). Mammalian ATPase II is found in chromaffin granules (Zachowski et al., 1989), synaptic vesicles (Hicks and Parsons, 1992), and clathrin-coated vesicles (Xie et al., 1989), although the function of ATPase II in these vesicles is not known. While there is no evidence that Drs2p generates phospholipid asymmetry in the yeast plasma membrane, the *drs2Δ* mutant has been reported to exhibit a defect in translocation of a fluorescent PS derivative across the plasma membrane (Tang et al., 1996). However, this result has been disputed (Siegmund et al., 1998), calling into question whether Drs2p functions as an aminophospholipid translocase at the plasma membrane.

In addition to the synthetic lethal interaction with *arf1Δ*, we found that *drs2Δ* also exhibits a specific synthetic lethal interaction with *chc1-ts* alleles. Moreover, the *drs2Δ* mutant has a defect in late Golgi function and exhibits several phenotypes at the nonpermissive temperature that suggest a loss of clathrin function at the yeast Golgi in vivo. Consistent with these observations, immunofluorescence and subcellular fractionation studies indicate that Drs2p localizes to late Golgi membranes. These results argue that the primary site of Drs2p function is in the Golgi complex rather than the plasma membrane, and suggest a link between Drs2p and the ARF-dependent recruitment of clathrin to Golgi membranes.

Materials and Methods

Strains and Media

Yeast cells were grown in standard rich medium (YPD), sporulation, or SD minimal media containing required supplements and 0.2% yeast extract where indicated (Sherman, 1991). Strains used were SEY6210 (*MATα leu2-3,112 ura3-52 his3-Δ200 trp1-Δ901 lys2-801 suc2-Δ9*; Robinson et al., 1988), 6210 *drs2Δ* (SEY6210 *drs2Δ*::TRP1), 6210 *arf1Δ* (SEY6210 *arf1Δ::HIS3*; Gaynor et al., 1998), 6210 *chc1-ts* (SEY6210 *chc1-ts::URA3*; Chen and Graham, 1998), PRY6222 (*MATa leu2-3,112 ura3-52 his3*-Δ200 *trp1-Δ901 ade 2-101 suc2-Δ9 drs2Δ::TRP1*), GPY1103 (*MATa leu2-3,112 ura3-52 his4-519 trp1 can1 chc1*-Δ8::LEU2; Payne et al., 1987), EGY101-16D (*MATa leu2-3,112 ura3-52 his3-Δ200 trp1-Δ901 suc2-Δ9* ret1-1; Gaynor et al., 1998), LSY93.1-10A (*MATα leu2-3,112 ura3-52 trp1* suc2 *clc1Δ::HIS3*; Chu et al., 1996), EGY1211-6B (*MATa leu2-3,112 ura3-52 his3-Δ200 trp1-Δ901 lys2-801 suc2-Δ9 sec21-1*; Gaynor et al., 1998), TBY103 (*MATa leu2-3,112 ura3-52 his3-Δ200 trp1-Δ901 sec23-1*), TGY144 (*MATα leu2-3,112 ura3-52 his3-Δ200 trp1-Δ901 lys2-801 sec1-1*), TGY1906 (*MATa leu2-3,112 ura3-52 his3-Δ200 trp1-Δ901 suc2-Δ9 pan1-20*), TGY1912 (*MATa leu2-3,112 ura3-52 his3-Δ200 trp1-Δ901 lys2-801 suc2-Δ9 end4-1*), SEY5185 (*MATa leu2-3,112 ura3-52 sec18-1*), BHY161 (SEY6210 *vps21Δ::HIS3*), BHY163 (SEY6210 *ypt7Δ::HIS3*), 6210 *vps33Δ* (SEY6210 *vps33Δ::HIS3*), and 6210 *vps35Δ* (SEY6210 *vps35Δ::HIS3*).

Cloning of SWA3 and Plasmid Construction

To clone *SWA3*, strain CCY2808 (*swa3-2*; Chen and Graham, 1998) was transformed with a genomic library (Horazdovsky et al., 1994) and Leu^+ transformants were selected on synthetic dextrose-Leu media containing 4 μg/ml adenine. After 7–10 d of incubation at 30°C, 50 colonies that appeared to sector (out of 21,000 transformants) were streaked on 5′-fluoroorotic acid (FOA) plates. Library plasmids were rescued from the four strains that grew on FOA and were retransformed into CCY2808. Only the transformants harboring pPR10 were able to sector on YPD at 30°C and were able to grow at 20°C. Partial sequencing indicated that the other three plasmids contained *ARF2*.

pPR10 contained a fragment of chromosome I from coordinates 94916–104338. Deletion of the BamHI fragment contained solely in *DRS2* (to produce pPR10ΔBamHI) destroyed the complementing activity of pPR10. The full-length *DRS2* gene contained on a SpeI-SnaBI fragment was subcloned into SpeI-SnaBI digested pRS315 or pRS425 to produce pRS315-DRS2 and pRS425-DRS2. Both plasmids complemented the cold-sensitive growth defect of CCY2808. A *drs2* deletion plasmid (pGCR1) was constructed by replacing a BamHI-SnaBI fragment in pPR10 with an ~1.1-kb BamHI-PvuII fragment containing *TRP1* from pJJ280 (Jones and Prakash, 1990). The plasmid pGCR1 was linearized with SacI and HpaI and transformed into SEY6210 to produce 6210 *drs2Δ*. The correct integration event was confirmed by PCR.

Site-directed mutagenesis of *DRS2* was performed by the megaprimer PCR method (Barik and Galinski, 1991). To generate megaprimers coding for either a D to N or D to E mutation at amino acid position 560, reverse primers TCCTGTCTTGTTACTGAATATAT and TCCTGTCTTTTCACTGAATATAT, respectively, were combined with forward primer TTTGTCACCGTTGAATTAATC into a PCR reaction mixture containing pRS315-DRS2. The gel purified ~150-bp product was added to a second PCR reaction containing the reverse primer TTCATCATCCAATCTTTCCAG and pRS315-DRS2. The resulting ~650-bp products were digested with BspEI and BglII, and then ligated into BspEI/BglII cut pRS315-DRS2 to produce pDRS2(D560N) and pDRS2(D560E). Sequencing of the resulting plasmids indicated that the specific mutations had been introduced with no additional mutations.

The 2-μm KEX2HA plasmid was constructed by subcloning a SalI/EagI digestion fragment of pSN218 (Nothwehr et al., 1995), containing the KEX2-HA sequence, into SalI/EagI-digested pRS426 to produce p426KH. The HA.11 mouse monoclonal antibody (Covance) was used at a 1:250 dilution to detect Kex2-HA by immunofluorescence.

Cell Labeling and Ste3p Turnover

Cell labeling, immunoprecipitation (Gaynor and Emr, 1997), FM4-64 up-

take (Vida and Emr, 1995), and Ste3p turnover (Davis et al., 1993) experiments were performed as previously described. Ste3p-myc was detected with 9E10 c-myc antibody (Oncogene Research Products) and HRP-conjugated secondary antibodies (Jackson ImmunoResearch Laboratories, Inc.) followed by the enhanced chemiluminescence detection (Amersham Corp.).

Subcellular Fractionation and Preparation of Clathrin-coated Vesicles

Subcellular fractionation was performed as previously described (Phan et al., 1994), except that cells were converted to spheroplasts and washed twice in buffer containing 0.8 M sorbitol before lysing with a Dounce homogenizer in buffer A containing 0.1 mg/ml RNase A. The cells were preincubated for 1 h at 15° or 30°C, lysed, and subjected to centrifugation at 13,000 *g* and the resulting supernatant was then centrifuged at 100,000 *g*. Immunoblots bearing 20 μg of protein from each sample were probed with mouse antibodies to Chc1p (Lemmon et al., 1988), Aps1 and Aps2 (Phan et al., 1994), and ARF1 (Kahn et al., 1995). Clathrin-coated vesicles (CCVs) were prepared from SEY6210 and 6210 *drs2Δ* as previously described (Mueller and Branton, 1984). For 15°C-treated samples, cells from a 3-liter culture grown to 6–8 OD were collected, resuspended into 1 liter of pre-chilled fresh YPD, and incubated at 15°C for 1 h before further processing. After gel filtration chromatography, 1.2 ml of every other fraction (total 5 ml per fraction) from fractions 15–35 were precipitated with TCA (10% final concentration). The precipitates were resuspended in 50 μl Laemmli sample buffer, and one third of each sample was subjected to immunoblotting and probed with antibodies to Chc1p, Mnn1p (Graham et al., 1994), and Pep12p (Seaman et al., 1998).

Electron Microscopy

Spheroplasts were prepared for electron microscopy as previously described (Rieder et al., 1996) except that the initial glutaraldehyde fixation was overnight at 4°C. 50–60-nm sections were viewed on an electron microscope (CM12; Philips). Vesicle fractions were similarly prepared, but included the following modifications: 5-ml fractions were fixed overnight at 4°C by addition of 700 μl of 25% glutaraldehyde (3% final concentration). Fixed vesicles were pelleted at 100,000 *g* for 70 min. The vesicle pellet was washed in 100 mM sodium cacodylate, pH 6.8, 5 mM $CaCl_2$, and then stained identically to the cell blocks, with one exception. A 30-min room temperature incubation with 1% tannic acid in 100 mM sodium cacodylate, pH 7.4, was included before en bloc staining with uranyl acetate. Dehydration, embedding, and section poststaining were performed as for the cell samples.

Preparation of Antiserum Against Drs2p

A *TrpE-DRS2* fusion construct was prepared by ligating the BglII/HindIII cut *DRS2* fragment (1,180 bp) from pPR10 into the BamHI/HindIII-digested pATH2 vector (Koerner et al., 1991). The resulting plasmid contained an in-frame fusion between TrpE and a region of Drs2p (amino acids 528–920) carrying ATPase motifs and predicted to be a cytoplasmic loop. This plasmid was transformed into JM101 cells and the resulting fusion protein was expressed and purified by the method of Koerner et al. (1991), except that the procedure was scaled up 10-fold to increase yield. Also, cracking buffer (10 mM sodium phosphate, pH 7.2, 1% β-mercaptoethanol, 1% SDS, 6 M urea) (Kleid et al., 1981) was used together with sonication to resuspend the insoluble portion of the total cell lysate before separation by preparative SDS-PAGE. The band from the preparative gel corresponding to the TrpE/Drs2 fusion protein was cut out and electroeluted using an Elutrap (Schleicher & Schuell, Inc.). Polyclonal rabbit antiserum to the Drs2-TrpE fusion protein was prepared at Scantibodies Laboratory. Drs2p antibodies were affinity purified twice as described (Pringle et al., 1991) using 500 μg of gel purified TrpE/Drs2 fusion protein bound to an Immobilon (Millipore Corp.) strip by capillary action. Affinity-purified anti–Drs2p antibody was used at a concentration of 1:1,000 for immunofluorescence and 1:2,000 for Western blots. Cell lysates for Western blots were prepared by vortexing cells with glass beads in SDS-urea sample buffer (40 mM Tris-HCl, pH 6.8, 8 M urea, 0.1 mM EDTA, 1% β-mercaptoethanol, 5% SDS) and heating at 50°C for 5 min. Boiling of samples caused aggregation of Drs2p such that the protein would remain in the stacking gel during SDS-PAGE.

Results

drs2Δ Is Synthetically Lethal with arf1Δ and chc1-ts Alleles

To clone the *SWA3* gene, a yeast genomic library (*CEN, LEU2*) was used to transform the *swa3-1* mutant, and the transformants were screened for complementation of the cold-sensitive growth and *arf1Δ* synthetic lethal phenotypes. A single library plasmid was isolated that was able to complement both mutant phenotypes and further subcloning analyses revealed that a 5-kb SpeI-SnaBI genomic fragment containing the full-length *DRS2* gene (and no other open reading frame, ORF) retained the complementing activity (see Materials and Methods).

A *drs2* null strain was generated by replacing most of the *DRS2* coding sequences with *TRP1*. Consistent with the phenotype previously reported for *drs2Δ* strains (Ripmaster et al., 1993) and that exhibited by the *swa3* mutants (Chen and Graham, 1998), the *drs2Δ* null mutant was unable to grow at 20°C or below, but grew well at temperatures above 23°C. Linkage analysis indicated that *SWA3* is allelic to *DRS2*, and synthetic lethality between *arf1Δ* and *drs2Δ* was confirmed by crossing the single mutants and characterizing the progeny by tetrad analysis (Fig. 1 A and data not shown). This genetic interaction suggested that Drs2p may be involved in an ARF-dependent vesicle-mediated protein transport event(s).

To determine if *drs2Δ* would exhibit synthetic lethality with other mutations that perturb transport vesicle formation, we crossed *drs2Δ* with strains harboring ts mutations in subunits of COPI (*ret1-1*, *sec21-1*, and *sec27-1* encoding α, γ, β′-COP, respectively), the ER transport vesicle coat

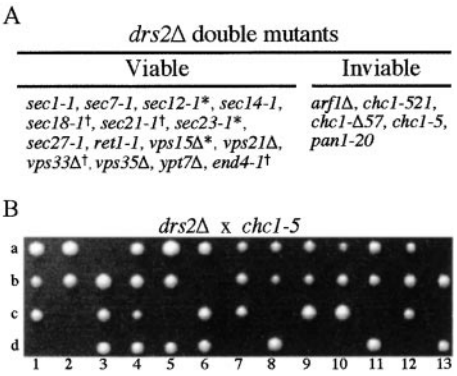

Figure 1. *drs2Δ* is synthetically lethal with *arf1Δ*, *chc1*, and *pan1* alleles. (A) Genetic analyses between *drs2Δ* and mutations that perturb the secretory pathway. Strains carrying the indicated mutations (see Materials and Methods) were crossed with a *drs2Δ* mutant (6210 *drs2Δ* or PRY6222) to generate diploids. After tetrad analyses of the progeny, the viable double mutants were streaked at 20°, 26.5°, and 37°C to compare the growth relative to parental strains carrying single mutations. *Double mutants of the alleles and *drs2* that were able to grow at 20°C, where single *drs2* mutants could not. †Double mutants that grew more slowly than either single mutant at 26.5°C. (B) Tetrad analysis of progeny derived from crossing PRY6222 (*drs2Δ*) with 6210 *chc1-5* (*chc1-5*). Spores that failed to grow were predicted to be *drs2Δ chc1-5* double mutants.

COPII (*sec12-1* and *sec23-1*), and the clathrin heavy chain (*chc1-5*, *chc1*-Δ57, *chc1-521*), and analyzed the progeny by tetrad dissection. All of the *sec drs2Δ* and the *ret1 drs2Δ* double mutants were obtained at the expected frequency (approximately one fourth of the progeny) and most grew well at 26.5°C (Fig. 1 A). The exception was *sec21-1 drs2Δ* mutants, which grew somewhat more slowly at this temperature than either single mutant. Among those growing well at 26.5°C, double mutants harboring *drs2Δ* and *sec12-1* or *sec23-1* also grew at 20°C, which is a nonpermissive temperature for *drs2Δ* single mutants. This suggests that *sec12* and *sec23* are able to partially suppress the cold-sensitive growth defect of *drs2Δ*, and that COPII may act upstream of Drs2p.

In stark contrast, *chc1-ts drs2Δ* double mutants were nearly always inviable. All of the spores that failed to grow in the tetrad analysis shown in Fig. 1 B were predicted to be *chc1-5 drs2Δ* double mutants based on the genotype of the viable spores from each tetrad. The *drs2Δ* and *chc1-5* single mutants grew nearly as well as wild-type progeny at this temperature (26.5°C, Fig. 1 B; e.g., spores 3c, 3d, and 3b are *drs2Δ*, *chc1-5*, and wild-type, respectively). Microscopic examination of the plates indicated that the *drs2Δ* chc1-5 spores germinated and divided a few times to form microcolonies, indicating that mitotic growth, rather than germination, was impaired. In addition, this genetic interaction was not allele-specific since all three of the *chc1* ts alleles tested were synthetically lethal with *drs2Δ* (Fig. 1 A).

To further address the specificity of the synthetic lethal interaction between *drs2Δ*, *arf1Δ*, and *chc1-ts* alleles, we crossed *drs2Δ* with several mutants that exhibit a defect in protein transport through the secretory or endocytic pathways. Double mutants combining *drs2Δ* with *sec1-1*, *sec7-1*, *sec14-1*, *sec18-1*, *vps15Δ*, vps21Δ, vps33Δ, vps35Δ, *ypt7Δ*, or *end4-1* were obtained at the expected frequency, although the *end4-1 drs2Δ*, *vps33Δ drs2Δ*, and *sec18-1 drs2Δ* mutants exhibited a slow growth phenotype. Interestingly, a mutant allele of the yeast Eps15 homologue, *pan1-20*, was also synthetically lethal with *drs2Δ* (Fig. 1 A). Eps15 is a cytoplasmic protein that localizes to clathrin-coated pits and may have an adaptor-like function in clathrin coated vesicle formation (van Delft et al., 1997; Wendland and Emr, 1998). Of particular note was the lack of genetic interactions with *sec7* and *sec14*, which both perturb protein transport through the yeast Golgi complex.

The drs2Δ Mutant Secretes Pro–α-Factor at the Nonpermissive Temperature

One of the more striking phenotypes of yeast clathrin mutants is the mislocalization of several late Golgi (TGN) proteins that are required for pro–α-factor proteolytic processing. This results in the secretion of fully glycosylated pro–α-factor rather than the mature peptide (Payne and Schekman, 1989). If clathrin function at the TGN is perturbed in the *drs2Δ* mutant, we would expect this mutant to secrete pro–α-factor. To test this, wild-type, *drs2Δ*, and *clc1Δ* (clathrin light chain null) strains were grown at 30°C, and after shifting to 20°C for 1 h, were metabolically labeled and chased at this nonpermissive temperature for *drs2Δ*. Aliquots of cells were removed at the chase times

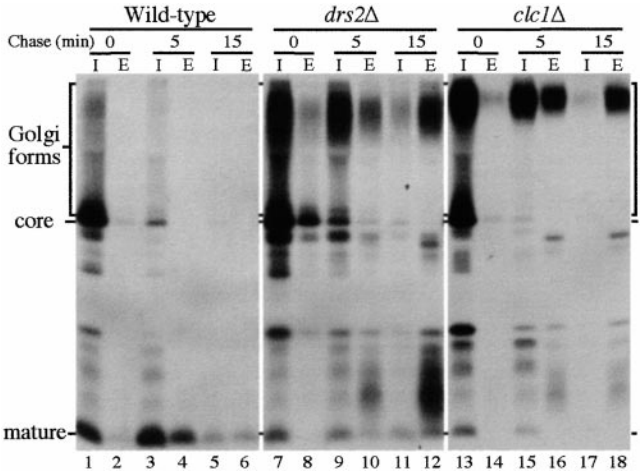

Figure 2. The *drs2Δ* mutant exhibits a cold-sensitive defect in pro–α-factor processing. Wild-type, *drs2Δ* (hereafter used to represent SEY6210 and the isogenic strain 6210 *drs2Δ*, respectively), and *clc1*Δ (LSY93.1-10A) strains were labeled for 10 min at 15°C, chased for the times indicated, and converted to spheroplasts. Intracellular (I) and extracellular (E) portions were separated by centrifugation and subjected to immunoprecipitation with antiserum to α-factor.

indicated in Fig. 2, converted to spheroplasts, and then centrifuged to separate intracellular (I) from extracellular (E) fractions. α-Factor was then recovered from each sample by immunoprecipitation.

At the beginning of the chase, labeled α-factor was present throughout the secretory pathway of the cells, as indicated by the presence of the core glycosylated ER proform, Golgi-modified hyperglycosylated proforms and the mature form (Fig. 2, lanes 1, 7, and 13). In wild-type cells, complete proteolytic processing of pro–α-factor occurred within 15 min, and most of the mature α-factor was secreted and degraded in the extracellular space. However, the *clc1Δ* cells were clearly deficient in the processing of pro–α-factor, and most of the hyperglycosylated precursor was secreted into the extracellular space within 15 min, as previously reported (Fig. 2, lane 18; Chu et al., 1996). Similarly, the *drs2Δ* mutant secreted the hyperglycosylated pro–α-factor and partially processed α-factor forms into the extracellular space (Fig. 2, lanes 10 and 12). The *drs2Δ* mutant also exhibited a modest defect in Golgi-specific glycosylation since the hyperglycosylated pro–α-factor secreted from *drs2Δ* cells showed a slightly faster mobility within the SDS-polyacrylamide gel relative to that from the *clc1*Δ strains. The kinetics of pro–α-factor secretion at this temperature (20°C) was nearly equivalent to that of *clc1Δ* cells. These results indicate that late Golgi function is specifically perturbed in the *drs2Δ* cells and suggest a loss of clathrin function at the TGN at the nonpermissive temperature. In pulse–chase experiments performed at 30°C, most of pro–α-factor was processed and secreted as the mature form from *drs2Δ* cells (data not shown), indicating that this defect was temperature conditional. Moreover, the pro–α-factor processing defect was observed within 15 min of preincubation at 20°C, suggesting a rapid onset of the temperature conditional phenotype (data not shown).

The drs2Δ Mutant Exhibits an Endosomal Defect

To examine protein transport through the endocytic pathway of *drs2Δ* cells, we followed the turnover of the α-factor receptor, Ste3p, which is constitutively endocytosed and delivered to the yeast vacuole where it is degraded (Davis et al., 1993). A c-myc tagged Ste3p expressed from a galactose-regulated promoter (Davis et al., 1993) was used so new Ste3p synthesis can be shut off by shifting the cells to glucose. Wild-type, *drs2Δ*, and *arf1Δ* cells were grown in galactose at 30°C to induce expression of the construct and populate the plasma membrane with the Ste3-myc protein. Glucose was added to the culture, which was then shifted to 15°C, and the disappearance of Ste3-myc was followed over time by immunoblotting. Even though the *arf1Δ* mutant displays an abnormal endosome morphology (Gaynor et al., 1998), the kinetics of Ste3p transport to the vacuole as measured by Ste3-myc degradation was very similar to that of wild-type cells (Fig. 3 A, *arf1Δ*). In contrast, the rate of Ste3-myc turnover was three- to fivefold slower in the *drs2Δ* cells (Fig. 3 A, *drs2Δ*) compared with wild type, suggesting a defect in endocytosis. To control for recovery of protein in each sample, the same blots were probed for carboxypeptidase Y (CPY), which was recovered equally in each sample (data not shown). *drs2Δ* cells cultured in glucose did not express Ste3p-myc, indicating that glucose repression of the *GAL* promoter was not perturbed (data not shown). Again, this phenotype was temperature conditional since the rate of Ste3-myc turnover at 30°C in the *drs2Δ* strain was only slightly (1.4-fold) slower than the wild-type strain (data not shown).

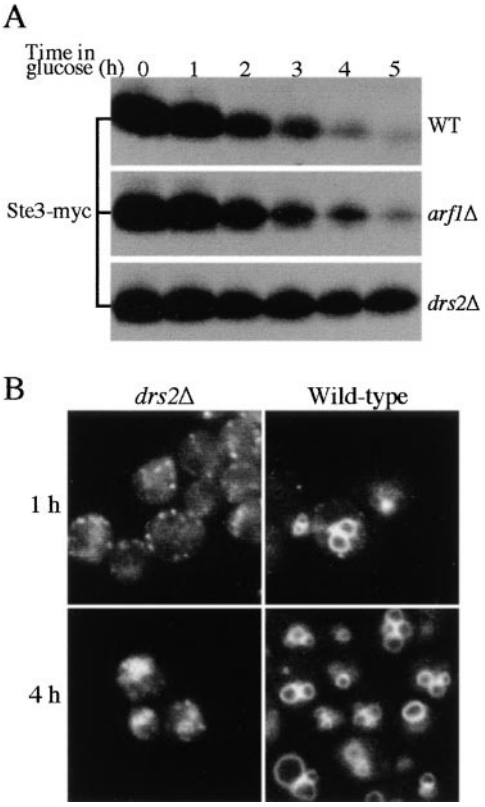

Figure 3. The *drs2Δ* mutant exhibits a cold-sensitive defect in the endocytic pathway. (A) Wild-type, *drs2Δ*, and *arf1Δ* strains were transformed with a plasmid carrying the Ste3-myc construct (pSL2624; Givan and Sprague, 1997) and grown to early log phase in galactose to induce expression of the STE3-myc protein. Glucose was added to 3% final concentration to repress new synthesis of Ste3-myc and the cultures were shifted to 15°C. Lysates were prepared at the times indicated and immunoblotted for Ste3-myc using the 9E10 c-myc antibody. (B) Wild-type and *drs2Δ* cells were stained with FM4-64 on ice and shifted to 15°C to initiate endocytosis of the dye. Images were captured at 1 and 4 h after shift to 15°C.

Clathrin mutants display a similar defect in Ste3p turnover caused by inefficient internalization of the receptor from the plasma membrane (Tan et al., 1993). However, examination of *drs2Δ* cells by immunofluorescence localization of Ste3p-myc at each time point after glucose was added indicated an accumulation of Ste3-myc in intracellular structures with very little plasma membrane staining (data not shown). This result suggested that transport of Ste3p from the endosome to the vacuole, rather than internalization from the plasma membrane, was perturbed.

To more specifically test whether uptake from the plasma membrane or transport from endosomes to the vacuole was defective in *drs2Δ* cells at the nonpermissive temperature, we stained cells with the fluorescent endocytic marker FM4-64 (Vida and Emr, 1995) on ice, and then shifted the cultures to 15°C to initiate endocytosis of the dye (Fig. 3 B). The FM4-64 was rapidly cleared from the plasma membrane of both wild-type and *drs2Δ* cells (data not shown), and in wild-type cells it was delivered to the vacuole membrane in 30–60 min (WT, 1 h). In contrast, the FM4-64 accumulated in endosomes of *drs2Δ* cells, which appear as punctate fluorescent spots in Fig. 3 B (*drs2Δ*, 1 h). Even after 4 h at 15°C, most of the FM4-64 was not in the vacuoles and stained what appeared to be clusters of smaller structures (*drs2Δ*, 4 h). As the *drs2Δ* cells warmed up on the microscope stage, the FM4-64 was rapidly delivered to the vacuoles at all times tested, indicating that the defect was fully reversible (data not shown). In addition, vacuoles in *drs2Δ* cells that were stained with FM4-64 at 30°C did not appreciably fragment when the cells were shifted to 15°C (data not shown), so the structures stained at 15°C were indeed endosomes and not fragmented vacuoles.

These studies indicated that the endocytic defect observed in *drs2Δ* cells was attributable to a defect in the endosome-to-vacuole pathway rather than clathrin-dependent endocytosis from the plasma membrane. If so, CPY transport should be affected as well since this protein follows a TGN to endosome to vacuole delivery route. To test this, we examined the transport of CPY to the vacuole in the *drs2Δ* mutant. CPY is synthesized in the ER as the p1 precursor form and is modified on N-linked oligosaccharides by the Golgi α1,3 mannosyltransferase (Mnn1p) to form the p2 precursor. p2 CPY is sorted from secreted proteins in the TGN and ultimately processed to the mature form in the vacuole (Stevens et al., 1982). Wild-type, *drs2Δ*, and *arf1Δ* cells were pulse-labeled and chased at either the permissive or nonpermissive temperature of *drs2Δ*. Aliquots of cells were removed at the chase times indicated and CPY was recovered by immunoprecipitation. As shown in Fig. 4, *drs2Δ* cells displayed near wild-

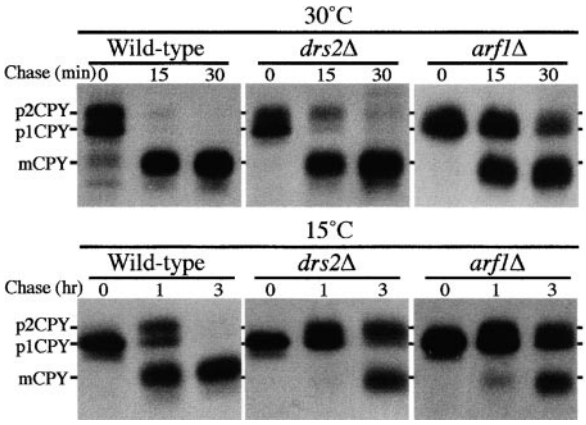

Figure 4. The *drs2Δ* mutant exhibits a cold-sensitive kinetic defect in CPY transport to the vacuole. Wild-type, *drs2Δ*, and *arf1Δ* (all isogenic to SEY6210) strains were labeled for 10 min at 15° or 30°C, and then chased for the times indicated. CPY was recovered from each sample by immunoprecipitation and subjected to SDS-PAGE.

type CPY transport kinetics at 30°C, while at 15°C the transport of CPY in *drs2Δ* mutants was significantly delayed relative to that in the wild-type cells, and was similar to the defect observed in *arf1Δ* cells at either temperature (approximately threefold slower transport kinetics). The partial glycosylation defect observed in *drs2Δ* (and *arf1Δ* cells) prevented the formation of a p2 CPY form that could be resolved from the p1 form in SDS-polyacrylamide gels. Thus, the kinetics of ER-to-Golgi transport could not be assessed for CPY. However, the ER-to-Golgi transport kinetics for α-factor and invertase in *drs2Δ* cells was found to be nearly wild type at the nonpermissive temperature, as scored by disappearance of the ER core form (Fig. 2, and data not shown). Therefore, it is unlikely that ER-to-Golgi transport for CPY is disturbed in *drs2Δ* cells. These data are most consistent with the interpretation that protein transport from the late Golgi or endosomes to the vacuole is perturbed by the *drs2Δ* mutation. Interestingly, the *chc1-5* allele isolated in the *arf1Δ* synthetic lethal screen also exhibits a partial glycosylation defect and an approximately threefold slower transport kinetics for CPY (Chen and Graham, 1998).

The drs2Δ Mutant Accumulates Abnormal Membrane-bound Structures Similar to Berkeley Bodies

Most of the *sec* mutants that exhibit a temperature-conditional block in protein transport also accumulate an organelle or vesicular intermediate of the secretory pathway at the nonpermissive temperature. For example, the *sec7*

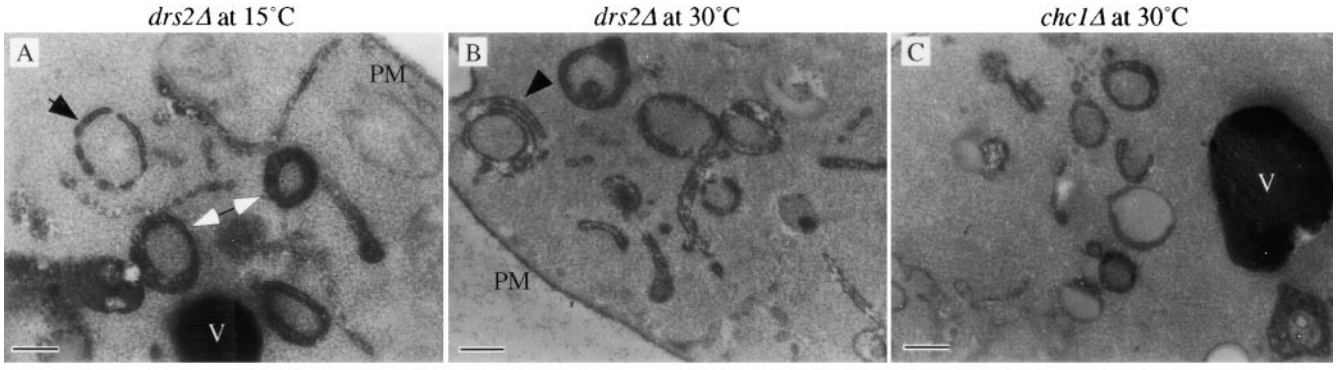

E

		Structures/cell section			
		Crescents +	Rings =	Total	Vesicles
Wild-type	37°	0.18	0.00	0.18	0.76
	26.5°	0.17	0.13	0.30	0.35
	20°	0.08	0.23	0.31	0.73
drs2Δ	37°	0.28	0.40	0.68	0.92
	26.5°	0.84	1.43	2.27	0.73
	20°	0.48	1.92	2.40	0.48

Figure 5. The *drs2Δ* mutant accumulates abnormal membrane structures that are similar to Berkeley bodies. Electron micrographs of *drs2Δ* cells incubated for 2 h at 15°C (A) or kept at 30°C (B) showing numerous double-membrane ring and crescent-shaped structures. Plasma membrane (PM) and vacuoles (V) are labeled. The black arrowhead in A denotes a modestly fenestrated ring structure. The arrowhead in B shows a ring structure with a stacked crescent membrane. For comparison, an electron micrograph of similar structures observed in a *chc1Δ* cell (C, GPY1103) is shown. Narrower, more fenestrated, and typically incomplete ring structures were also found in wild-type (WT) cells grown at 30°C (D, arrowhead). These wild-type ring structures did not stain as darkly as rings found in the *drs2Δ* mutant (compare to double arrowhead in A). Bars, 0.2 μm. E, *drs2Δ* and wild-type cells grown at the indicated temperatures were visualized by transmission electron microscopy. Membrane bound structures from 23–25 randomly selected cells were counted and expressed as an average number of structures per cell section.

and *sec14* mutations block protein transport out of the Golgi complex and accumulate Golgi structures called Berkeley bodies (Novick et al., 1980). The Golgi cisternae in these mutants are sometimes stacked and appear to adopt a deep, cup-shaped morphology that in electron micrographs of thin sections present double-membrane ring or crescent shaped structures depending on the section plane. Clathrin mutants also exhibit aberrant membrane structures similar to Berkeley bodies, although these structures are rarely stacked (Payne et al., 1987).

Morphological studies by electron microscopy revealed that *drs2Δ* cells accumulated aberrant double-membrane ring and crescent-shaped structures at both 15° and 30°C (Fig. 5, A and B). The double-membrane rings in the *drs2Δ* cells measured 200–250 nm in diameter (average, 240 nm) and often presented a significant gap between the concentric membranes, which should be equivalent to the luminal space of the cisternae. Representative double-membrane ring structures are marked with white arrowheads in Fig. 5 A. Very similar ring structures also accumulated in the *chc1*Δ mutant (Fig. 5 C; Payne et al., 1987). These types of structures were never observed in wild-type cells; however, ring structures could be found that were more highly fenestrated and appeared to be breaking down into tubules or vesicles (Fig. 5 D, arrowhead). In fact, similar fenestrated ring structures accumulate dramatically in *arf1Δ* cells (Gaynor et al., 1998). Some of the double-membrane rings in the *drs2Δ* cells were also modestly fenestrated (Fig. 5 A, black arrow).

To quantitate the effect of temperature on the accumulation of ring structures in wild-type and *drs2Δ* cells, these cells were grown at 26.5°C and shifted to the temperature indicated in Fig. 5 E for 2 h before fixation. Regions containing 23–25 cell sections were randomly selected and the number of crescent-shaped structures, double-membrane rings, and vesicles (50–100-nm spheres) were counted and expressed as the number of structures per cell section. Relative to the wild-type strain, the *drs2Δ* mutant accumulated four- to eightfold more crescent and ring structures at the temperatures examined (Fig. 5 E). In this analysis, structures similar to that shown in Fig. 5 D were counted as rings in the wild-type cells. There was also a greater accumulation of these structures in the *drs2Δ* cells at the colder temperatures, which was particularly evident for the double-membrane rings. The number of vesicles in the *drs2Δ* cells dropped modestly at the colder temperatures, although within the range of values observed for the wild-type cells.

Golgi membranes that accumulate at the nonpermissive temperature in the *sec7* mutant have been reported to become more extensively stacked in low glucose medium (Novick et al., 1980). Some structures appear stacked in the *drs2Δ* mutant grown in 2% glucose (Fig. 5 B, arrow), but no significant difference was observed in the morphology of the membranes accumulating in *drs2Δ* cells incubated in low glucose (0.1%) medium for 2 h at the nonpermissive temperature. However, the effect of low glucose on Berkeley body structure in a *sec7* mutant in our strain background was modest (data not shown).

Plasma membrane invaginations have been proposed to represent endocytic intermediates in yeast (Mulholland et al., 1999) and are extended in some mutants that exhibit a defect in endocytosis [for example, *sjl1 sjl2* (Srinivasan et al., 1997) and *pan1* (Wendland et al., 1996)]. However, no difference in the depth of plasma membrane invaginations between wild-type and *drs2Δ* cells was observed under any of the growth conditions described above.

Reduction of Intact Clathrin-coated Vesicles that Can Be Isolated from the drs2Δ Mutant

A mammalian cytosolic ARF guanine nucleotide exchange factor requires both PS and phosphatidylinositol-4,5-bisphosphate for optimal membrane binding and subsequent activation of ARF (Chardin et al., 1996). This observation suggested a requirement for Drs2p (a potential PS translocase) to recruit ARF and clathrin to membranes. To test whether Drs2p plays a role in regulating ARF activation and therefore association of ARF and clathrin with membranes, we fractionated both wild-type and *drs2Δ* cellular lysates by differential centrifugation to compare the amounts of ARF, clathrin, and adaptin subunits recovered in the 13,000-*g* pellets, and the 100,000-*g* pellets and supernatants. A small increase in the amount of clathrin heavy chain found in the 100,000-*g* supernatant fraction was occasionally observed in the mutant samples relative to the wild-type samples at both 15° and 30°C; otherwise, the fractionation pattern for clathrin was very similar between the two strains (data not shown). In addition, the fractionation pattern for ARF and the two adaptin small subunits (Aps1p for AP-1 and Aps2p for AP-2) was nearly identical between *drs2Δ* and wild-type samples. Therefore, the association of ARF and clathrin with bulk cellular membranes seemed to be unaffected in the *drs2Δ* mutant, although we cannot rule out the possibility that the distribution of ARF between specific organelles is perturbed.

To further assess clathrin function in the *drs2Δ* mutants, we asked whether CCVs could be purified from this mutant. CCV preparations were generated from *drs2Δ* and wild-type cells with or without a 1-h shift to 15°C (see Materials and Methods). Cell lysates were centrifuged at 21,000 *g* for 30 min to pellet large organellar membranes (e.g., plasma membrane, vacuolar membrane, ER, and mitochondria) and the resulting supernatant was centrifuged at 100,000 *g* to pellet vesicles. The 100,000-*g* pellet was then applied to a Sephacryl S-1000 gel filtration column (Mueller and Branton, 1984), and the fractions were probed for the clathrin heavy chain by immunoblotting. As shown in Fig. 6 A, the clathrin heavy chain was highly enriched in fractions 23 to 27 for both wild-type and *drs2Δ* samples from cells shifted to 15°C (Fig. 6 A) or 30°C (Fig. 7 D, and data not shown). In addition, from Coomassie blue–stained gels, we estimated that the recovery of clathrin heavy chain in these fractions was comparable for both strains at both temperatures (data not shown).

However, a clear difference between wild-type and mutant samples was evident when fractions highly enriched for the clathrin heavy chain were examined by EM. Peak clathrin fractions obtained from wild-type cells were substantially enriched in CCVs with a clear lipid bilayer present in a substantial number of the vesicle profiles (Fig. 6 C, arrowheads). In contrast, most of the vesicle profiles in the *drs2Δ* peak clathrin fractions contained an electron

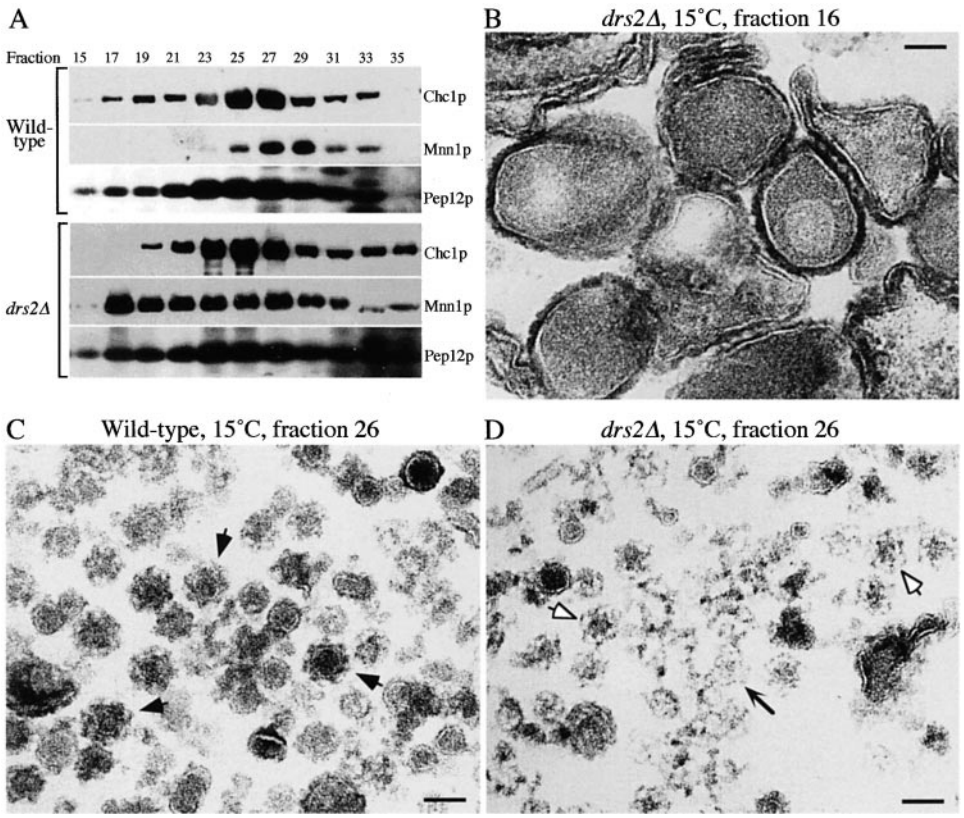

Figure 6. The *drs2Δ* mutant accumulates aberrant Golgi membranes and exhibits a deficiency of clathrin-coated vesicles. (A) Wild-type and *drs2Δ* cells were grown at 30°C and shifted to 15°C for 1 h, and then lysed and subjected to centrifugation at 21,000 *g* for 30 min. The 21,000-*g* supernatant was centrifuged at 100,000 *g* for 80 min to generate a 100,000-*g* pellet. This pellet was resuspended and further resolved on a Sephacryl S-1000 column. Samples of every other fraction from fraction 15 to 35 were assayed by immunoblotting for the clathrin heavy chain (Chc1p), a late Golgi protein Mnn1p, and an endosomal t-SNARE Pep12p. (B–D) Membranes in fraction 16 from the *drs2Δ* sample where Mnn1p was found (B), and fraction 26 from wild-type (C) and *drs2Δ* (D) samples where Chc1p was enriched were fixed, pelleted, and examined by EM. Bars, 50 nm.

dense center, but no lipid bilayer within the clathrin basket (Fig. 6 D, open arrowheads). In addition, the *drs2Δ* fractions contained what appeared to be partially assembled clathrin lattices (Fig. 6 D, arrow) that were rarely observed in wild-type fractions. CCVs with a lipid bilayer were occasionally observed in the *drs2Δ* fractions, but were found at <1/10 of the frequency per section as compared with the wild-type samples (multiple sections from three different preparations were compared). This was a temperature-conditional phenomenon as CCV preparations from *drs2Δ* cells maintained at a permissive temperature were indistinguishable from wild-type samples (data not shown).

It is well established that clathrin triskelions can self assemble into baskets in slightly acidic, low ionic strength buffers (Schmid, 1997, and references therein). The method we used for isolating CCVs from yeast applies such buffer conditions to retain assembled coats on vesicles. In addition, the lysate is incubated for 30 min at 30°C with RNase to reduce the amount of ribonucleoprotein complexes in the P100 sample. These conditions are likely to induce assembly of free clathrin triskelions into baskets and lattices within the *drs2Δ* cell lysate. It appears that these clathrin structures pellet at 100,000 *g* and elute from the S-1000 column in similar fractions as bona fide CCVs. The simplest interpretation of these data is that the *drs2Δ* cells are deficient in producing CCVs at the nonpermissive temperature. It is also possible that clathrin dissociates more readily from CCVs produced in *drs2Δ* cells and reassembles into baskets during purification, thus preventing the isolation of bona fide CCVs. In either case, there is a marked difference between *drs2Δ* and wild-type cells either in the ability to produce CCVs or in the physical properties of CCVs from these strains.

Even though most large membranes pellet at 21,000 *g*, we had noticed by EM that the 100,000-*g* pellet from *drs2Δ* cells (that was applied to the S1000 column) contained a significant number of aberrant membrane structures that were similar in appearance and size to those observed in cell sections (Fig. 5 B). Because *drs2Δ* cells exhibited both Golgi and endosome-associated defects, it was possible that both organelles would accumulate in the *drs2Δ* mutant. Therefore, we examined the S1000 column fractions from the CCV preparations for membranes containing a late Golgi protein, α1,3-mannosyltransferase (Mnn1p), and an endosomal t-SNARE, Pep12p (Fig. 6 A). In fractions from wild-type cells, Mnn1p eluted slightly later than clathrin, which likely represents small vesicles or small Golgi fragments. However, a substantial change in the elution profile of Mnn1p-containing membranes was observed in fractions from *drs2Δ* cells. A peak of Mnn1p eluted just after the void volume and spread from fractions 16–31. This change in Mnn1p distribution was observed with samples prepared from *drs2Δ* cells incubated at both 15°C (Fig. 6 A) and 30°C (data not shown), and correlated with the large membrane structures observed by EM in these fractions (e.g., Fig. 6 B, fraction 16). Membranes of any sort were difficult to find by EM in fraction 16 from wild-type samples (data not shown). Relative to Mnn1p, a wider distribution of Pep12p-containing membranes was found in the S1000 fractions from wild-type cells. However, the Pep12p elution profile was not significantly

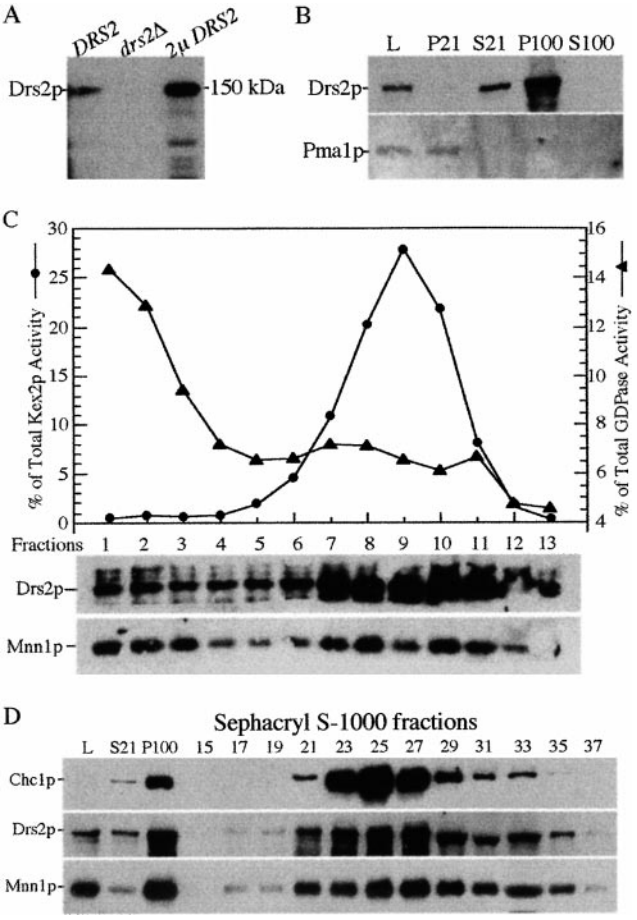

Figure 7. Drs2p cofractionates with high-density membranes containing the late Golgi markers, Kex2p and Mnn1p. (A) Specificity of the Drs2p antibodies. Wild-type, *drs2Δ*, and SEY6210 pRS425-DRS2 (*2*μ DRS2) cells were grown at 30°C before lysing with glass beads in SDS-urea sample buffer. Total cellular proteins (0.1 OD per lane) were subjected to SDS-PAGE and immunoblotted with affinity-purified antibodies against Drs2p. (B) Wild-type cells grown at 30°C were lysed (lysate, L) and subjected to centrifugation at 21,000 *g* for 30 min to generate pellet (P21) and supernatant (S21) fractions. The S21 fraction was further centrifuged at 100,000 *g* for 80 min to generate pellet (P100) and supernatant (S100) fractions. 20 μg of total protein per fraction was immunoblotted for Drs2p and the plasma membrane ATPase, Pma1p. (C) Wild-type cells grown at 30°C were lysed and subjected to differential centrifugation and sucrose gradient fractionation of the P100 fraction. These gradient fractions have been previously used to examine Mnn1p distribution in Figure 6 a of Reynolds et al. (1998). Equal volumes per gradient fraction were assayed by enzyme activity for Kex2p or GDPase and by immunoblotting for Drs2p, Mnn1p, and Pep12p. (D) Wild-type cells were grown at 30°C, lysed, and subjected to differential centrifugation to produce a P100 fraction, which was then subjected to gel filtration chromatography as described in Fig. 6. Samples of every other fraction from fraction 15 to 35 were assayed by immunoblotting for the clathrin heavy chain (Chc1p), the late Golgi protein Mnn1p and Drs2p.

different between the wild-type and *drs2Δ* fractions (Fig. 6 A). These data suggest that the abnormal membrane structures that accumulate in the *drs2Δ* cells are Golgi membranes and not endosomal membranes.

Drs2p Localizes to Late Golgi Membranes Containing Kex2p and Mnn1p

To analyze the intracellular localization of Drs2p, we prepared a rabbit polyclonal antiserum against a bacterially expressed fragment of Drs2p (amino acid residues 528–920). Affinity-purified anti–Drs2p antibodies recognized an ~150-kD protein on an immunoblot of a wild-type cell lysate (Fig. 7 A, *DRS2*), which is in close agreement to the predicted mass of 154 kD. This protein was not present in a *drs2Δ* cell lysate and was found in greater abundance in wild-type strain carrying *DRS2* on a multicopy plasmid (Fig. 7 A, *drs2Δ* and *2* μ DRS2). Thus, the 150-kD protein is equivalent to Drs2p.

Drs2p was recently suggested to localize to the plasma membrane based on cofractionation of an epitope-tagged Drs2p with the plasma membrane ATPase, Pma1p, in sucrose gradient fractions from a crude cell lysate (Siegmund et al., 1998). However, we found that membranes containing Drs2p could be quantitatively separated from membranes containing Pma1p by differential centrifugation as described above for the CCV preparations. Equal amounts of protein from the lysate (L), pellet (P21), and supernatant (S21) of 21,000 *g* and pellet (P100) and supernatant (S100) of 100,000 *g* were probed for Drs2p and Pma1p. Nearly all of Drs2p remained in the supernatant after centrifuging at 21,000 *g* (S21) while most of Pma1p was found in the pellet (P21) (Fig. 7 B). All of the Drs2p in the S21 was pelleted during the subsequent 100,000-*g* centrifugation step and was found in the P100 fraction.

The fractionation profile for Drs2p shown in Fig. 7 B is very similar to how CCV and late Golgi proteins such as Kex2p fractionate. To further characterize the localization of Drs2p, a P100 fraction was applied to the bottom of a sucrose gradient and centrifuged to equilibrium (Reynolds et al., 1998). Fractions were collected from the top and probed for Drs2p and Mnn1p and assayed for GDPase and Kex2p (Fig. 7 C). GDPase marks early Golgi compartments, Kex2p the late Golgi (or TGN), and Mnn1p is typically split between these two regions of the gradient. The fractionation pattern for Drs2p clearly matches that of Kex2p (Fig. 7 C). In similar gradients, we found that the endosomal marker Pep12p was broadly distributed throughout the gradient (data not shown), although others have observed a defined peak in fractions significantly lighter than that of Kex2p (Becherer et al., 1996). In no case did the Pep12p fractionation pattern match with that of Drs2p. In addition, the S1000 column elution profile of membranes containing Drs2p (from wild-type cells grown at 30°C) matched that of membranes containing Mnn1p (Fig. 7 D). The Drs2p elution profile overlapped that of CCVs (Fig. 7 D), raising the possibility that some Drs2p is present within the CCVs. This possibility is currently being tested; however, it appeared that the bulk of Drs2p resides in Golgi membranes.

To determine whether Drs2p and Kex2p reside in the same membrane structures, wild-type cells overexpressing a hemagglutinin (HA)-tagged Kex2p were stained simultaneously with antibodies to Drs2p and HA. Localization of Drs2p by immunofluorescence produced a punctate staining pattern that is typical for the yeast Golgi complex (Fig. 8, WT + 2μ KEX2HA, α-Drs2p). Although the sig-

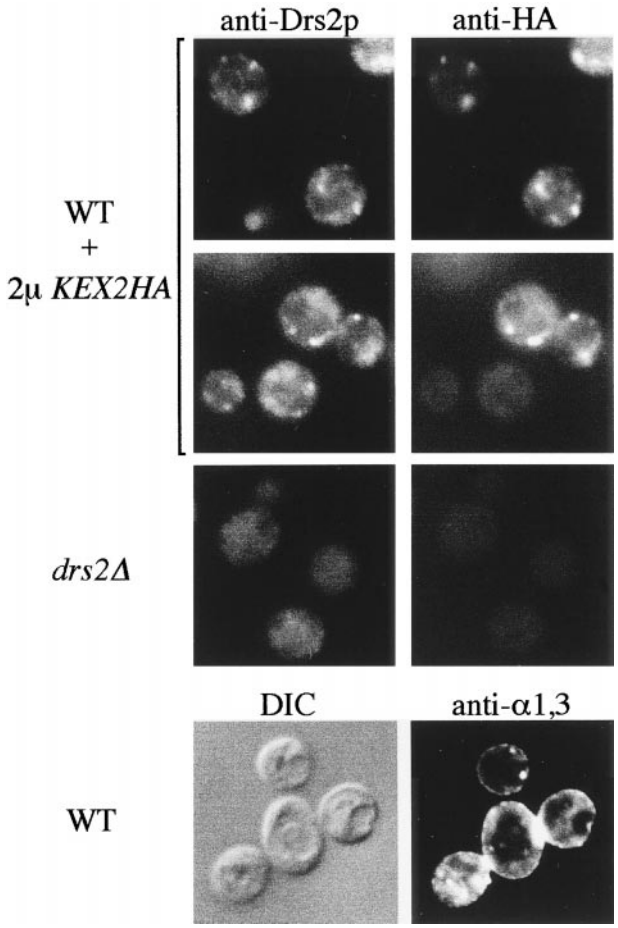

Figure 8. Drs2p colocalizes with Kex2p in internal, punctate membranes. The wild-type strain carrying the HA-tagged *KEX2* on a 2-μm plasmid (WT + 2μ KEX2HA), and the *drs2Δ* strain were grown overnight at 30°C in minimal medium. After dilution in rich medium to 0.2 OD_{600}, the wild-type strain was shifted to 20°C and cultured for 7 h while the *drs2Δ* strain was cultured at 30°C for 5 h, and then shifted to 20°C for 2 h. Cells were then fixed and prepared for immunofluorescence as previously described (Graham et al., 1994). Affinity-purified anti–Drs2p and monoclonal anti–HA antibodies were used in the top six panels to visualize Drs2p (left) and the HA-tagged Kex2p (right) in the same cells. The bottom two panels are DIC and immunofluorescence images of wild-type cells grown at 20°C and labeled with an antibody specific for α1,3-linked mannose. Notice how the punctate and rim staining pattern (plasma membrane) of α1,3-mannose epitopes is different from the punctate staining of Drs2p in wild-type cells.

nal was weak, it was clearly above the background staining observed for the *drs2Δ* strain (Fig. 8, *drs2Δ*). The HA antibody also produced a punctate staining pattern (Fig. 8, WT + 2μ KEX2HA, α-HA) and, importantly, most of the structures that were positive for Drs2p also stained for Kex2-HA. As expected, very little overlap was observed between Drs2p and the early Golgi marker Och1-HA (data not shown).

We could not detect plasma membrane staining with the Drs2p antibodies, which is inconsistent with a previous report suggesting that Drs2p resides in the plasma membrane (Siegmund et al., 1998). Overexpression of Drs2p from a multicopy plasmid resulted in an ER staining pattern (Siegmund et al., 1998, and data not shown), so this method could not be used to enhance the signal. To determine whether the lack of plasma membrane staining with Drs2p antibodies was due to a technical limitation, we tested whether we could detect plasma membrane staining for an antigen that is present in the Golgi, endosomes, and plasma membrane. Wild-type spheroplasts were stained with antibodies to α1,3-linked mannose residues that are found on many glycoproteins. For these cells, staining of the plasma membrane is clearly observed as a stained rim around the cells (Fig. 8, anti–α1,3). Thus, by both immunofluorescence and subcellular fractionation studies, it appears that most, if not all, of Drs2p is found in late Golgi membranes.

Mutation of Aspartic Acid 560 Abolishes Drs2p Function In Vivo

Drs2p is predicted to be a P-type ATPase based on the presence of five well-conserved ATPase motifs involved in the binding and hydrolysis of ATP (Fig. 9 A). For P-type ATPases, an aspartic acid within the second motif forms an aspartyl-phosphate catalytic intermediate that is essential for ATP hydrolysis (Allen and Green, 1976; Fagan and Saier, 1994). Sequence alignments between Drs2p and other P-type ATPases predict that aspartic acid 560 (D560) in Drs2p would form the aspartyl-phosphate intermediate (Fig. 9 A). To test whether this amino acid is critical for Drs2p function, we mutated D560 to either an asparagine (D560N) or a glutamic acid (D560E) residue and examined the ability of the mutants to complement the cold-sensitive growth defect of the *drs2Δ* strain. These mutations would be expected to cause minimal structural

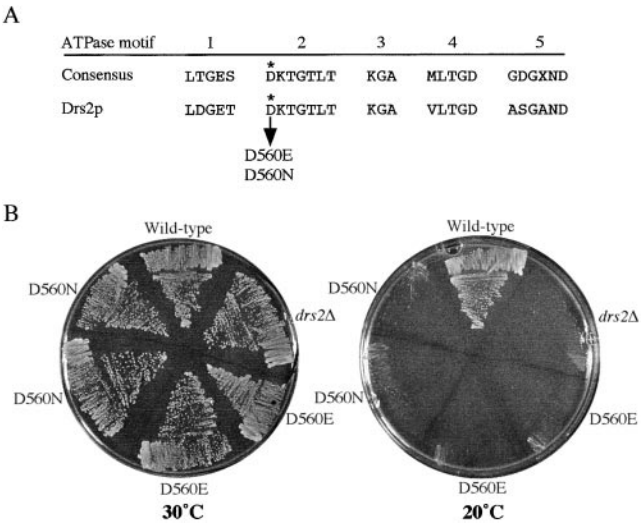

Figure 9. Mutation of a conserved ATPase motif causes loss of Drs2p function in vivo. (A) Comparison of five conserved consensus motifs of yeast P-type ATPases and the corresponding sequence in Drs2p (adapted from Catty et al., 1997). The arrow indicates the aspartic acid residue (D) at position 560, which was mutated to glutamic acid (E) or asparagine (N). (B) The *drs2Δ* strain containing plasmids pDRS2(D560E), pDRS2(D560N), pRS315-DRS2 (wild-type), and the pRS315 empty vector (*drs2Δ*) were grown at 30° or 20°C for 3 d.

changes in Drs2p, but should abolish the presumed ATPase activity of this protein. The *drs2Δ* strain carrying either the wild-type *DRS2* gene (Wild-type), an empty vector (*drs2Δ*), or two independent isolates of each mutant (D560N and D560E) were tested for growth at 30° and 20°C (Fig. 9 B). As previously reported, the *drs2Δ* strain failed to grow at 20°C, but grew well at 30°C. None of the strains carrying the D560 point mutations were able to grow at 20°C (Fig. 9 B), even though each of the strains expressed a wild-type level of Drs2p (data not shown). These data support the assignment of Drs2p as a P-type ATPase and suggest that the ATPase activity of Drs2p is essential for its function in vivo.

Discussion

In this report, we present several lines of evidence that strongly implicate the integral membrane P-type ATPase Drs2p in late Golgi function, and suggest a link between Drs2p and CCV formation from Golgi membranes. (a) A specific synthetic lethal interaction was found between *drs2Δ*, *arf1Δ*, and *chc1-ts* alleles. (b) The *drs2Δ* mutant exhibits a cold-sensitive defect in the proteolytic processing of pro–α-factor in the yeast TGN that is comparable with the defect shown by clathrin mutants. (c) The *drs2Δ* mutant accumulates aberrant Golgi structures that are morphologically comparable to the membrane structures that accumulate in clathrin mutants. (d) We observed a substantial decrease in the yield of CCVs that could be isolated from the *drs2Δ* mutant preincubated at the nonpermissive temperature. (e) Drs2p localizes to late Golgi membranes containing Kex2p.

Specific Genetic Interactions between drs2Δ, arf1Δ, and chc1-ts Alleles

Our rationale for performing the *arf1Δ* synthetic lethal screen was that it could provide an unbiased, in vivo approach to identify proteins that regulate ARF function, or participate with ARF in CCV or COPI vesicle formation. This was the first yeast genetic screen we are aware of that has uncovered a mutant allele of the clathrin heavy chain gene (*swa5-1/chc1-5*; Chen and Graham, 1998). While mutations at many loci can influence the viability of a *chc1Δ* strain (Munn et al., 1991), there are no other reports of mutations that are lethal in combination with *chc1-ts* alleles other than *arf1Δ*. This provides genetic support for the substantial biochemical evidence in the literature implicating ARF in clathrin recruitment to Golgi membranes (Zhu et al., 1998, and references therein), and also provides validation for the *arf1Δ* synthetic lethal approach.

We were initially concerned about the specificity of the *drs2Δ–arf1Δ* synthetic lethal interaction, even though four alleles of the *SWA3/DRS2* gene were recovered in this genetic screen. However, from crosses with 19 different mutants that perturb the secretory or endocytic pathways, we found a specific interaction between pairwise combinations of *arf1Δ*, *drs2Δ*, and *chc1-ts* alleles. The *drs2Δ* allele was also synthetically lethal with *pan1-20*, an eps15-related protein that interacts with yAP180 (yeast homologue of clathrin assembly protein AP180) in a yeast two-hybrid assay (Wendland and Emr, 1998). Importantly, there was no genetic interaction between *drs2Δ* and mutant ts alleles encoding three different COPI subunits, even though combination of *arf1Δ* with these COPI alleles produces a synthetic growth defect (Gaynor et al., 1998). These results suggest that Drs2p is specifically involved in clathrin, but not COPI, function. This interpretation is supported by the finding that membranes containing Drs2p could be separated from early Golgi membranes where COPI would be expected to function, and cofractionated with late Golgi membranes where clathrin function is required.

Phenotypes Exhibited by the drs2Δ Mutant

These genetic analyses prompted us to examine the *drs2Δ* mutant for defects in the secretory and endocytic pathways. The secretion kinetics and Golgi-specific glycosylation of pro–α-factor and invertase were only modestly perturbed. However, a substantial cold-sensitive defect in the Kex2p-dependent processing of pro–α-factor was observed. This resulted in secretion of the pro–α-factor precursor, a phenotype also exhibited by clathrin mutants (Payne and Schekman, 1989). Kinetic defects were also observed for CPY transport to the vacuole and the turnover of the Ste3p pheromone receptor within the vacuole. These phenotypes are likely caused by a delay in endosome-to-vacuole transport that was clearly observed using the fluorescent endocytic tracer FM4-64. Thus, the *drs2Δ* mutation seems to specifically perturb late Golgi (TGN) and endosome function.

As visualized by EM, the *drs2Δ* mutant accumulates abnormal membrane-bound structures that were morphologically equivalent to structures that accumulate in clathrin mutants. The abnormal membrane structures that were isolated from *drs2Δ* cells by differential centrifugation and gel exclusion chromatography were enriched for a late Golgi protein, but not for an endosomal marker protein. Since the localization studies suggest that Drs2p is a late Golgi (TGN) resident, these data strongly suggest that Drs2p acts in the late Golgi to maintain normal structure and function of this compartment. It is possible that Drs2p has some function in the endosome as well, or the effect on endosome function could be a secondary consequence of perturbing late Golgi function.

Perhaps the most compelling evidence that Drs2p plays a role in clathrin function is the striking difference in the appearance of CCV preparations between *drs2Δ* and wild-type cells. Very few bona fide CCVs could be isolated from *drs2Δ* cells preincubated at the nonpermissive temperature. These preparations contained clathrin baskets and lattices with no associated membrane. In contrast, CCV preparations from *drs2Δ* cells maintained at 30°C were indistinguishable from wild-type samples. These results suggest that Drs2p is required to form clathrin-coated vesicles from Golgi membranes at temperatures below 23°C. However, it is also possible that the association of clathrin coats with vesicle membranes from *drs2Δ* cells is less stable and the coat dissociates during cell lysis. In either case, loss of Drs2p clearly perturbs CCVs.

At this time, it is not possible to distinguish whether the effect of Drs2p on clathrin function is direct or a secondary consequence of the abnormal TGN structure. However, this effect is specific since the TGN of *drs2Δ* cells

functions normally in the ability to sort vacuolar proteins and in protein secretion, despite the abnormal morphology. This suggests that late secretory vesicles bud normally from the TGN in *drs2Δ* cells. The genetic interactions also showed a high degree of specificity between *drs2Δ* and clathrin mutations. Therefore, there is not a wholesale loss of Golgi function in *drs2Δ* cells at the nonpermissive temperature. Indeed, most of the specific defects observed can be explained by a loss of clathrin function. Even the accumulation of abnormal membrane at the permissive temperature could be the result of inefficient CCV budding.

The temperature-conditional defects observed for a strain carrying a complete loss of function allele is somewhat unusual. This suggests that Drs2p is required to overcome an inherently cold-sensitive process in the cell (perhaps CCV budding), such that the growth defect is caused by the combination of low temperature and loss of Drs2p. However, this cold-sensitive process is not at the extreme of the normal growth range for yeast; *drs2Δ* cells fail to grow at room temperature (20°C) and the mutant phenotypes described here are observed at this temperature. In addition, some of the *drs2Δ* phenotypes, such as *arf1Δ* synthetic lethality and abnormal Golgi morphology, are also observed at 30°C. Thus, it appears that Drs2p plays a role in Golgi function at all temperatures examined but is only essential below 23°C. Alternatively, it is possible that Drs2p function is essential at all temperatures, but loss of Drs2p is compensated by one or more of the Drs2p-related P-type ATPases at higher temperatures. In either case, Drs2p clearly plays a critical role for organisms such as yeast since the ability to adapt to daily fluctuations in temperature is essential for their survival.

Potential Function of Drs2p as an Aminophospholipid Translocase

What is the biochemical function of Drs2p? Many P-type ATPases use the energy of ATP hydrolysis to pump cations such as Ca^{2+}, H^+, Na^+, or heavy metals across a membrane against their electrochemical gradient. These transporting ATPases contain signature motifs that allowed the identification of 16 P-type ATPases in the yeast genome that can be phylogenetically grouped into six distinct families (Catty et al., 1997). Four of the families correspond to the cation transporters just described, one family contains two ORFs of unknown function, and the last family are potential aminophospholipid transporters, which includes Drs2p and four other uncharacterized ORFs. Drs2p is 28–35% identical to its four other yeast family members, but is 47% identical to bovine or murine ATPase II from chromaffin granules (FASTA comparisons), arguing that Drs2p and ATPase II are orthologues. The closest related P-type ATPases to the Drs2p family are the Ca^{2+} transporters (21% identity between Drs2p and Pmc1p). However, Drs2p and ATPase II are missing negatively charged amino acids in transmembrane domains 4 and 6 that are essential for cation transport and have hydrophobic residues in their place. This is consistent with the proposed role of ATPase II and Drs2p in transporting aminophospholipids and makes it less likely that Drs2p transports cations.

The *drs2Δ* mutant has been reported to exhibit a defect in the translocation of a fluorescent PS derivative across the plasma membrane (Tang et al., 1996). However, Siegmund et al. (1998) have recently challenged this observation and have failed to detect a difference between wild-type and *drs2Δ* cells in the translocation of fluorescent lipid derivatives across the plasma membrane. This group also found no difference in the amount of PE exposed on the outer leaflet of the plasma membrane as detected by trinitrobenzene sulfonic acid labeling. These latter observations could suggest that Drs2p is not an aminophospholipid translocase, but it is more likely that the Drs2p protein is simply not present at the plasma membrane and therefore is not required to maintain an asymmetric distribution of aminophospholipids in this membrane. In fact, we cannot detect Drs2p at the plasma membrane by immunofluorescence localization or subcellular fractionation (Figs. 7 and 8). Measurement of translocase activity with Golgi membrane fractions is more complicated because the direction of flip is expected to be from the luminal to the cytoplasmic leaflet and thus requires incorporation of the probe into the luminal leaflet. Thus, further work is required to determine if Drs2p is an aminophospholipid translocase, as suggested by its homology to ATPase II.

Since an aminophospholipid translocase activity is the only biochemical function attributed to ATPase II and Drs2p in the literature, it is relevant to speculate on how membrane asymmetry may affect Golgi structure and perhaps clathrin function. The bilayer couple hypothesis of Sheetz and Singer (1974) proposes that asymmetric changes in the two leaflets of a bilayer should induce conformational changes in the membrane. In fact, induced bilayer asymmetry can cause conversion of spherical liposomes into tubular and interconnected vesicular structures (Farge and Devaux, 1992). In this regard, it is possible that changes in the asymmetric distribution of PS or PE could influence the formation of tubules or fenestrated regions of Golgi cisternae to produce a structure on which clathrin can assemble more productively. This is consistent with the morphological defect observed for Golgi membranes in the *drs2Δ* mutant, which are notable for their lack of fenestration or tubular regions. Particularly in comparison to the *arf1Δ* mutant in which the Golgi is highly fenestrated or tubular in appearance (Gaynor et al., 1998).

Others have proposed that the transbilayer movement of lipid could induce the bending of membranes to facilitate vesicle budding (Devaux, 1991). Zha et al. (1998) have reported that changes in the composition of the plasma membrane outer leaflet caused by sphingomyelinase treatment can induce an energy-independent budding of functional endocytic vesicles. In addition, Farge et al. (1999) have recently reported that exogenous PS incorporated into the external leaflet of the plasma membrane was pumped to the inner leaflet and markedly enhanced the level of bulk endocytosis. Thus, it is feasible that Drs2p actively participates in CCV budding from Golgi membranes, and becomes essential for this process as the temperature drops below a specific threshold where a decreased fluidity of the membrane may prevent clathrin from performing this function alone.

A third possibility is that an increase in the PE or PS concentration of the cytoplasmic leaflet may influence the

recruitment or activity of peripherally associated proteins. For example, the association of an ARF guanine nucleotide exchange factor with Golgi membranes might be influenced by the PS concentration (Chardin et al., 1996). In addition, clathrin can be recruited on chemically defined liposomes, but requires an unusually high concentration of PE (40% of total lipid) to produce well-defined clathrin-coated buds on the membranes (Takei et al., 1998). One might expect that an enzyme that pumps PE to the cytoplasmic membrane could produce a high local concentration of this lipid, particularly if the coat proteins restrict lateral diffusion of PE. Purification and reconstitution of Drs2p in chemically defined liposomes will help define the biochemical function of this protein and perhaps shed light on how Drs2p influences clathrin function in vivo.

We thank Scott Emr, Richard Kahn, Sandra Lemmon, Greg Payne, Erin Gaynor, Bruce Horazdovsky, Beverly Wendland, and Todd Brigance for antibodies, strains, or plasmids. We thank Todd Reynolds for providing sucrose gradient fractions (for Fig. 7 C). We are particularly grateful to Guang-Ming Wu, Sidney Fleischer, and Paula Flicker for assistance with electron microscopy. We also thank Greg Payne, Sandra Lemmon, and members of the Graham lab for their helpful comments during the course of these experiments.

This work was supported by grants from the National Science Foundation (MCB-9600835, BIR-9419667) to T.R. Graham.

Submitted: 11 May 1999
Revised: 5 November 1999
Accepted: 9 November 1999

References

Allen, G., and N.M. Green. 1976. A 31-residue tryptic peptide from the active site of the [Ca^{++}]-transporting ATPase of rabbit sarcoplasmic reticulum. *FEBS Lett.* 63:188–192.

Auland, M.E., B.D. Roufogalis, P.F. Devaux, and A. Zachowski. 1994. Reconstitution of ATP-dependent aminophospholipid translocation in proteoliposomes. *Proc. Natl. Acad. Sci. USA*. 91:10938–10942.

Barik, S., and M.S. Galinski. 1991. Megaprimer method of PCR: increased template concentration improves yield. *Biotechnology*. 10:489–490.

Becherer, K.A., S.E. Rieder, S.D. Emr, and E.W. Jones. 1996. Novel syntaxin homologue, Pep12p, required for the sorting of lumenal hydrolases to the lysosome-like vacuole in yeast. *Mol. Biol. Cell.* 7:579–594.

Catty, P., A. de Kerchove d'Exaerde, and A. Goffeau. 1997. The complete inventory of the yeast *Saccharomyces cerevisiae* P-type transport ATPases. *FEBS Lett.* 409:325–332.

Chardin, P., S. Paris, B. Antonny, S. Robineau, S. Beraud-Dufour, C.L. Jackson, and M. Chabre. 1996. A human exchange factor for ARF contains Sec7- and pleckstrin-homology domains. *Nature.* 384:481–484.

Chen, C.-Y., and T.R. Graham. 1998. An *arf1Δ* synthetic lethal screen identifies a new clathrin heavy chain conditional allele that perturbs vacuolar protein transport in *Saccharomyces cerevisiae*. *Genetics.* 150:577–589.

Chu, D.S., B. Pishvaee, and G.S. Payne. 1996. The light chain subunit is required for clathrin function in *Saccharomyces cerevisiae*. *J. Biol. Chem*. 271: 33123–33130.

Davis, N.G., J.L. Horecka, and D.F. Sprague, Jr. 1993. Cis- and trans-acting functions required for endocytosis of the yeast pheromone receptors. *J. Cell Biol.* 122:53–65.

Devaux, P.F. 1991. Static and dynamic lipid asymmetry in cell membranes. *Biochemistry*. 30:1163–1173.

Fagan, M.J., and M.H. Saier, Jr. 1994. P-type ATPases of eukaryotes and bacteria: sequence analyses and construction of phylogenetic trees. *J. Mol. Evol.* 38:57–99.

Farge, E., and P.F. Devaux. 1992. Shape changes of giant liposomes induced by an asymmetric transmembrane distribution of phospholipids. *Biophys. J.* 61: 347–357.

Farge, E., D.M. Ojcius, A. Subtil, and A. Dautry-Varsat. 1999. Enhancement of endocytosis due to aminophospholipid transport across the plasma membrane of living cells. *Am. J. Physiol.* 276:C725–C733.

Gaynor, E.C., C.-Y. Chen, S.D. Emr, and T.R. Graham. 1998. ARF is required for maintenance of yeast Golgi and endosome structure and function. *Mol. Biol. Cell.* 9:653–670.

Gaynor, E.C., and S.D. Emr. 1997. COPI-independent anterograde transport: cargo-selective ER to Golgi protein transport in yeast COPI mutants. *J. Cell Biol.* 136:789–802.

Givan, S.A., and G.F. Sprague, Jr. 1997. The ankyrin repeat-containing protein Akr1p is required for the endocytosis of yeast pheromone receptors. *Mol. Biol. Cell.* 8:1317–1327.

Graham, T.R., M. Seeger, G.S. Payne, V. MacKay, and S.D. Emr. 1994. Clathrin-dependent localization of α1,3 mannosyltransferase to the Golgi complex of *Saccharomyces cerevisiae*. *J. Cell Biol.* 127:667–678.

Hicks, B.W., and S.M. Parsons. 1992. Characterization of the P-type and V-type ATPases of cholinergic synaptic vesicles and coupling of nucleotide hydrolysis to acetylcholine transport. *J. Neurochem*. 58:1211–1220.

Horazdovsky, B.F., G.R. Busch, and S.D. Emr. 1994. *VPS21* encodes a rab5-like GTP binding protein that is required for the sorting of yeast vacuolar proteins. *EMBO (Eur. Mol. Biol. Organ.) J.* 13:1297–1309.

Jones, J.S., and L. Prakash. 1990. Yeast *Saccharomyces cerevisiae* selectable markers in pUC18 polylinkers. *Yeast.* 6:363–366.

Kahn, R.A., J. Clark, C. Rulka, T. Stearns, C.J. Zhang, P.A. Randazzo, T. Terui, and M. Cavenagh. 1995. Mutational analysis of *Saccharomyces cerevisiae ARF1*. *J. Biol. Chem*. 270:143–150.

Kleid, D.G., D. Yansura, B. Small, D. Dowbenko, M. Moore, M.G. Grubman, P.D. McKercher, D.O. Morgan, B.H. Robertson, and H.L. Bachrach. 1981. Cloned viral protein vaccine for foot and mouth disease: responses in cattle and swine. *Science.* 214:1125–1129.

Koerner, T.J., J.E. Hill, A.M. Myers, and A. Tzagoloff. 1991. High-expression vectors with multiple cloning sites for construction of trpE fusion genes: pATH vectors. *Methods Enzymol.* 194:477–490.

Lemmon, S., V.P. Lemmon, and E.W. Jones. 1988. Characterization of yeast clathrin and anticlathrin heavy-chain monoclonal antibodies. *J. Cell. Biochem*. 36:329–340.

Lemmon, S.K., C. Freund, K. Conley, and E.W. Jones. 1990. Genetic instability of clathrin-deficient strains of *Saccharomyces cerevisiae*. *Genetics.* 124:27–38.

Mueller, S.C., and D. Branton. 1984. Identification of coated vesicles in *Saccharomyces cerevisiae*. *J. Cell Biol.* 98:341–346.

Mulholland, J., J. Konopka, B. Singer-Kruger, M. Zerial, and D. Botstein. 1999. Visualization of receptor-mediated endocytosis in yeast. *Mol. Biol. Cell.* 10: 799–817.

Munn, A.L., L. Silveira, M. Elgort, and G.S. Payne. 1991. Viability of clathrin heavy-chain–deficient *Saccharomyces cerevisiae* is compromised by mutations at numerous loci: implications for the suppression hypothesis. *Mol. Cell. Biol.* 11:3868–3878.

Nothwehr, S.F., E. Conibear, and T.H. Stevens. 1995. Golgi and vacuolar membrane proteins reach the vacuole in *vps1* mutant yeast cells via the plasma membrane. *J. Cell Biol.* 129:35–46.

Novick, P., C. Field, and R. Schekman. 1980. Identification of 23 complementation groups required for post-translational events in the yeast secretory pathway. *Cell.* 21:205–215.

Payne, G.S., D. Baker, E. van Tuinen, and R. Schekman. 1988. Protein transport to the vacuole and receptor-mediated endocytosis by clathrin heavy chain–deficient yeast. *J. Cell Biol.* 106:1453–1461.

Payne, G.S., T.B. Hasson, M.S. Hasson, and R. Schekman. 1987. Genetic and biochemical characterization of clathrin-deficient *Saccharomyces cerevisiae*. *Mol. Cell. Biol.* 7:3888–3898.

Payne, G.S., and R. Schekman. 1989. Clathrin: a role in the intracellular retention of a Golgi membrane protein. *Science.* 245:1358–1365.

Phan, H.L., J.A. Finlay, D.S. Chu, P.K. Tan, T. Kirchhausen, and G.S. Payne. 1994. The *Saccharomyces cerevisiae APS1* gene encodes a homolog of the small subunit of the mammalian clathrin AP-1 complex: evidence for functional interaction with clathrin at the Golgi complex. *EMBO (Eur. Mol. Biol. Organ.) J.* 13:1706–1717.

Pringle, J.R., A.E.M. Adams, D.G. Drubin, and B.K. Haarer. 1991. Immunofluorescence methods for yeast. *Methods Enzymol.* 194:565–602.

Rad, M.R., H.L. Phan, L. Kirchrath, P.K. Tan, T. Kirchhausen, C.P. Hollenberg, and G.S. Payne. 1995. *Saccharomyces cerevisiae* Apl2p, a homologue of the mammalian clathrin AP β subunit, plays a role in clathrin-dependent Golgi functions. *J. Cell Sci.* 108:1605–1615.

Reynolds, T.B., B.D. Hopkins, M.R. Lyons, and T.R. Graham. 1998. The high osmolarity glycerol response (HOG) MAP kinase pathway controls localization of a yeast Golgi glycosyltransferase. *J. Cell Biol.* 143:935–946.

Rieder, S.E., L.M. Banta, K. Kohrer, J.M. McCaffery, and S.D. Emr. 1996. Multilamellar endosome-like compartment accumulates in the yeast *vps28* vacuolar protein sorting mutant. *Mol. Biol. Cell.* 7:985–999.

Ripmaster, T.L., G.P. Vaughn, and J.L. Woolford, Jr. 1993. *DRS1* to *DRS7*, novel genes required for ribosome assembly and function in *Saccharomyces cerevisiae*. *Mol. Cell. Biol.* 13:7901–7912.

Robinson, J.S., D.J. Klionsky, L.M. Banta, and S.D. Emr. 1988. Protein sorting in *Saccharomyces cerevisiae*: isolation of mutants defective in the delivery and processing of multiple vacuolar hydrolases. *Mol. Cell. Biol.* 8:4936–4948.

Schmid, S.L. 1997. Clathrin-coated vesicle formation and protein sorting: an integrated process. *Annu. Rev. Biochem*. 66:511–548.

Seaman, M.N., J.M. McCaffery, and S.D. Emr. 1998. A membrane coat complex essential for endosome-to-Golgi retrograde transport in yeast. *J. Cell Biol.* 142:665–681.

Sheetz, M.P., and S.J. Singer. 1974. Biological membranes as bilayer couples. A molecular mechanism of drug–erythrocyte interactions. *Proc. Natl. Acad. Sci. USA*. 71:4457–4461.

Sherman, F. 1991. Guide to yeast genetics and molecular biology. *Methods En-*

zymol. 194:3–21.

Siegmund, A., A. Grant, C. Angeletti, L. Malone, J.W. Nichols, and H.K. Rudolph. 1998. Loss of Drs2p does not abolish transfer of fluorescence-labeled phospholipids across the plasma membrane of *Saccharomyces cerevisiae*. *J. Biol. Chem.* 273:34399–34405.

Srinivasan, S., M. Seaman, Y. Nemoto, L. Daniell, S.F. Suchy, S. Emr, P. De Camilli, and R. Nussbaum. 1997. Disruption of three phosphatidylinositol-polyphosphate 5-phosphatase genes from *Saccharomyces cerevisiae* results in pleiotropic abnormalities of vacuole morphology, cell shape, and osmo-homeostasis. *Eur. J. Cell Biol.* 74:350–360.

Stearns, T., R.A. Kahn, D. Botstein, and M.A. Hoyt. 1990a. ADP ribosylation factor is an essential protein in *Saccharomyces cerevisiae* and is encoded by two genes. *Mol. Cell. Biol.* 10:6690–6699.

Stearns, T., M.C. Willingham, D. Botstein, and R.A. Kahn. 1990b. ADP-ribosylation factor is functionally and physically associated with the Golgi complex. *Proc. Natl. Acad. Sci. USA.* 87:1238–1242.

Stepp, J.D., A. Pellicena-Palle, S. Hamilton, T. Kirchhausen, and S.K. Lemmon. 1995. A late Golgi sorting function for *Saccharomyces cerevisiae* Apm1p, but not for Apm2p, a second yeast clathrin AP medium chain-related protein. *Mol. Biol. Cell.* 6:41–58.

Stevens, T., B. Esmon, and R. Schekman. 1982. Early stages in the yeast secretory pathway are required for transport of carboxypeptidase Y to the vacuole. *Cell.* 30:439–448.

Takei, K., V. Haucke, V. Slepnev, K. Farsad, M. Salazar, H. Chen, and P. De Camilli. 1998. Generation of coated intermediates of clathrin-mediated endocytosis on protein-free liposomes. *Cell.* 94:131–141.

Tan, P.K., N.G. Davis, G.F. Sprague, Jr., and G.S. Payne. 1993. Clathrin facilitates the internalization of seven transmembrane segment receptors for mating pheromones in yeast. *J. Cell Biol.* 123:1707–1716.

Tang, X., M.S. Halleck, R.A. Schlegel, and P. Williamson. 1996. A subfamily of P-type ATPases with aminophospholipid transporting activity. *Science.* 272: 1495–1497.

van Delft, S., C. Schumacher, W. Hage, A.J. Verkleij, and P.M. van Bergen en Henegouwen. 1997. Association and colocalization of Eps15 with adaptor protein-2 and clathrin. *J. Cell Biol.* 136:811–821.

Vida, T.A., and S.D. Emr. 1995. A new vital stain for visualizing vacuolar membrane dynamics and endocytosis in yeast. *J. Cell Biol.* 128:779–792.

Wendland, B., and S.D. Emr. 1998. Pan1p, yeast eps15, functions as a multivalent adaptor that coordinates protein–protein interactions essential for endocytosis. *J. Cell Biol.* 141:71–84.

Wendland, B., J.M. McCaffery, Q. Xiao, and S.D. Emr. 1996. A novel fluorescence-activated cell sorter–based screen for yeast endocytosis mutants identifies a yeast homologue of mammalian eps15. *J. Cell Biol.* 135:1485–1500.

Williamson, P., and R.A. Schlegel. 1994. Back and forth: the regulation and function of transbilayer phospholipid movement in eukaryotic cells. *Mol. Membr. Biol.* 11:199–216.

Xie, X.S., D.K. Stone, and E. Racker. 1989. Purification of a vanadate-sensitive ATPase from clathrin-coated vesicles of bovine brain. *J. Biol. Chem.* 264: 1710–1714.

Zachowski, A., J.P. Henry, and P.F. Devaux. 1989. Control of transmembrane lipid asymmetry in chromaffin granules by an ATP-dependent protein. *Nature.* 340:75–76.

Zha, X., L.M. Pierini, P.L. Leopold, P.J. Skiba, I. Tabas, and F.R. Maxfield. 1998. Sphingomyelinase treatment induces ATP-independent endocytosis. *J. Cell Biol.* 140:39–47.

Zhu, Y., L.M. Traub, and S. Kornfeld. 1998. ADP-ribosylation factor 1 transiently activates high-affinity adaptor protein complex AP-1 binding sites on Golgi membranes. *Mol. Biol. Cell.* 9:1323–1337.